Real-Time Physical Model of a Piano-Hammer String Interaction Coupled to a Soundboard

F. Pfeifle
Hamburg University, Neue Rabenstr. 13, 20354 Hamburg, Germany
fpfeifle@gmail.com

A methodology and working implementation for synthesis of physical models, solved with symplectic and multi-symplectic finite difference algorithms running on a Field Programable Gate Array (FPGA), capable of auralising instrument models in real-time, presented by the author, is extended to synthesize the physical model of a grand piano-hammer/string-course interaction coupled to a soundboard. The piano hammer string interaction is modeled as a non-linear hysteretic impact model and iterated with a finite difference time domain integration scheme. The three strings of the course are iterated numerically with a symplectic Euler scheme time integrator and central finite difference approximation of the spatial domain. The soundboard is modeled as a 2-dimensional Kirchhoff plate with a non-linear normal load distiburtion resulting from the inclusion of a virtual piano bridge, and orthotropic material properties due to different Youngs moduli in the respective grain directions of the wood. The coupling between the strings and the soundboard is modeled by an impedance coupling at the interaction point, allowing vibrations from the soundboard to couple back to the strings, influencing the vibrations of the strings. The model is implemented on two XILINX ML605 FPGA development boards connected by a high speed IO port via the on-board SMA ports. The implementation is capable of auralising the sound radiated from the front plate and integrated to two virtual listener positions in real-time. It is possible to change physical parameters like the coupling strength, parameters of the hammer model, the tune of the strings and multiple others while playing.

1 Introduction

Physical modeling of the complete grand piano or single constituents of the instrument is an active field of research, especially over the last thirty years. Treatises regarding physical models of certain features of a piano are for instance the works of Bacon [30] , Boutillon [5], Chaigne [17]; [18], Chabassier [2]. Most of these works are based on the large body of research regarding the acoustical properties of the grand piano as well as the upright piano (see: [7, 6, 16]). Several works regarding physical models of pianos show that important features can be described satisfactorily with mathematical models (see for instance [3]) other mechanisms still escape a description, like for instance the exact role of the piano bridge and the influence on the string vibration [2], or the specific losses in the soundboard [19]. In many of these works, researchers are confronted by a multitude of different physical parameters influencing a certain part of a model. Because the computation time of physical models rises with its complexity, most numerical implementations of physical models are not capable of synthesizing sounds in real-time or even close to real-time.

In this work, a methodology for computing a finite difference physical model of certain aspects of the piano in real-time is presented. It is an initial effort to show the feasibility of calculating a physical model of a large instrument, such as the piano, on a Field Programmable Gate Array (FPGA). The implementation is based on a similar methodology, developed at the Institute of Systematic Musicology (Hamburg), for several lute instruments as presented by the author [10]. The physical model, presented in this work consists of a grand piano string course coupled to a wooden soundboard and a non-linear hammer impact, and is capable of auralising the synthesized sound in real-time. There are several related works regarding real-time physical models calculated on a FPGA like the work of Chen et al. [23], which presents a model to compute the 2-dimensional wave equation with a Finite Difference Time Domain (FDTD) scheme on a FPGA. A physical model of a single string computed in real-time on a FPGA is proposed by Gibbons et al. [22]. Other notable publications, regarding numerical calculation of the wave equation using finite difference methods are works by Motuk et al. [26, 27] where a FDTD algorithm is utilised to solve the 2-dimensional wave equation for membranes and plates.

2 Physical model

2.1 Piano-hammer-string interaction

The model of the piano hammer is based on a non-linear hammer-force/string interaction with hysteresis due to the compression characteristics of the felt covered hammer tip. The forces acting at the contact point between a piano hammer and a string course was subject to manifold research. Askenfeldt et al. researched the non-linear interaction between a piano hammer and a string with electrodynamic measurement techniques [7], Stulov utilised a device to measure the exerted force of the hammer and proposed an exact model of the non-linear hysteresis properties of the felt tip [12]. More recently, Birkett [11] showed the influence of the hammer-shank movement on the acting hammer force as well as an accurate measurement of the compression of the hammer felt, applying high-speed camera recordings and motion tracking methods. A comprehensive four parameter model of the force exerted by a piano hammer is proposed by Stulov [12]. This model was simplified in a later work [15] to a three parameter model, without a loss of accuracy inside the range of realistic hammer velocities below 10 $\frac{m}{s}$. It can be written as:

$$F_{contact} = -F_0 \left[(1 - \zeta)\, x^\gamma + \tau x_t^\gamma \right] \tag{1}$$

with ζ and τ the *hereditary* (state preserving) parameters of the hammer felt, γ a non-linear exponent depending on properties of the felt varying between 1.5 and 2.8 for new hammers, and 2.5 − 3.9 for used hammers.[29] x is the compression of the hammer tip felt due to the interaction with the string at the contact point, and F_0 the hammer stiffness. The subscript t indicates a differentiation by time.

2.2 String model

The transversal and the longitudinal motion of a linear string can be described by the 1-dimensional wave equation, also known as the d'Alembert equation. Inside a domain $\mathbf{x} \in 0, \cdots, L$ with the boundary conditions $u|_{x=0} = u|_{x=L} = 0$ the differential equation is given as:

$$\mathbf{u}_{tt} - c^2 \cdot \mathbf{u}_{xx} = 0 \tag{2}$$

with $\mathbf{u}$ the deflection in vectorial form, $c = \sqrt{\frac{T}{\mu}}$ the wave propagation speed, with T the tension applied to the string,

and μ the linear density. $\mathbf{u}_{xx}$ and $\mathbf{u}_{tt}$ indicate a second order differentiation by x and t respectively. For most stringed lute instruments, equipped with short and reasonably flexible strings, equation 2 suffices to describe the transverse motion of the string, which is the main mode of vibration radiated from most lute instruments.

In contrast to this, piano strings show characteristic effects not described by equation 2, which must be taken into account in a physical model. Because of their comparably large diameter and stiffness, which is due to the high string tension applied in pianos, two effects have an impact on the vibration of the strings: (a) The bending stiffness, giving the piano string a bar-like characteristic and giving rise to detuning [16], and (b) Longitudinal modes of the string, which have a noticeable influence on the perceived sound of the instrument [8]. The bending stiffness can be implemented by adding a fourth order beam-like term to equation 2

$$\mathbf{u}_{tt} - c^2 \cdot \mathbf{u}_{xx} + \kappa \cdot \mathbf{u}_{4x} = 0 \tag{3}$$

with $\kappa = \frac{ESK^2}{\mu}$ a factor consisting of the Young's Modulus E, the cross-sectional area S, the radius of gyration K, the linear density μ, and the subscript $4x$ indicating a fourth order differentiation in respect to x.

The longitudinal motion of the string also obeys equation 2. A geometrically correct interaction between the longitudinal and the transverse motion of the string is proposed in Chabassier et al. [2], taking the influence of the longitudinal motion on the tension of the string into account. In the model applied in this work, the variable tension effects are neglected and only the transversal to longitudinal coupling is implemented as a transversal deflection dependent excitation of the longitudinal motion as proposed Bank and Sujbert [24]. Resulting in the following formulation for the longitudinal deflection ξ:

$$\xi_{tt} = \frac{T}{\mu}\xi_{xx} + ES\frac{1}{2}[u_{xx}^2]_x \tag{4}$$

In addition to the bending stiffness and the longitudinal motion of the string, real piano strings are subject to several kinds of losses: a) velocity damping due to air friction, b) internal damping due to material imperfections, c) losses due to energy transfer at the bridge. The first two effects are included directly into the formulation of the differential equation as presented by Chaigne and Askenfelt in [17, 18]. An extension to the internal damping, also known as frequency dependent damping, is proposed by Bensa et al. [25]. The final form of the equation used to model the transversal motion of the string including all of the mentioned effects can be written as:

$$\mathbf{u}_{tt} = c^2 \cdot \mathbf{u}_{xx} - \kappa \cdot \mathbf{u}_{4x} - \beta\mathbf{u}_t - \alpha\mathbf{u}_{xxt}. \tag{5}$$

The last two terms indicate the velocity dependent damping and the frequency dependent damping with the two damping constants β and α. The values for β and α are taken from literature [25, 2].

2.3 Soundboard model

The piano soundboard amplifies the vibrational energy of the strings, which is transferred via the piano bridge. In upright pianos it has a rectangular shape, and a more difficile geometry in the case of a grand piano. The soundboard modeled in this work consists of several non-linearities like orthotropic material constants due to the physical properties of the utilised wood (Sitka spruce is utilised here), discontinuities at the edges of the individual planks, which are glued with animal glue, a non-linear distribution of stresses due to the crowning and the normal loads of the bass and treble bridge [19, 20].

The orthotropy of the material leads to different wave velocities in the respective grain directions, which are standardly denoted by V_L for the longitudinal, V_R for the radial and V_T for the transversal directions. The planks utilised for a piano soundboard are commonly a longitudinal/transversal cut and are selected on aesthetic grounds as well as the regularity of annual rings which can vary between 0.7 and 3 mm depending on the position in the instrument (see Bucur [21]). A few basic assumptions regarding the model of the soundboard are formulated upfront:

- The height of the soundboard, which is somewhere between $6 - 9$ mm, is small compared to the extent in the other two dimensions. Hence, it is reasonable to apply a 2-dimensional plate theory for a physical model.
- The deflection of the soundboard is small, meaning large amplitude effects can be left out of the consideration.
- Deformations due to transverse shear stresses included in the Reissner-Mindlin plate model, are not as important due to the small height of the plate. Therefore the Kirchhoff-Love plate theory can be applied.
- The ribs are included as additional masses and heights at the respective rib positions.
- The discontinuities at the glued ribs due to the high stiffness of animal glue are not taken into account.
- The normal force due to air loading is not taken into account in this model.

Using the constants from Table 1, the bending moments $\mathbf{M}$ on an orthotropic plate are given by following differential equations:

$$\begin{aligned} M^x &= -[D_x \cdot u_{xx} + D_{xy} \cdot u_{yy}] \\ M^y &= -[D_x \cdot u_{yy} + D_{xy} \cdot u_{xx}] \\ M^{xy} &= -2 \cdot D_s \cdot u_{xy}, \end{aligned} \tag{6}$$

Table 1: Orthotopic plate constants.

$D_x =$	$\frac{E_L}{1-\nu_L\nu_T}\frac{\tilde{h}^3}{12}$	$D_y =$	$\frac{E_T}{1-\nu_L\nu_T}\frac{\tilde{h}^3}{12}$
$D_{xy} =$	$\frac{E_L\nu_T}{1-\nu_L\nu_T}\frac{\tilde{h}^3}{12}$	$D_{yx} =$	$\frac{E_L\nu_T}{1-\nu_L\nu_T}\frac{\tilde{h}^3}{12}$
	$D_{sh} =$	$\frac{G\tilde{h}^3}{12}$	

G is the shear modulus and $\tilde{h} = h(x, y)$ the variable height of the plate, E are the Young's moduli and ν the Poisson ratios which depend on the elastic properties of the wood.

Using the shear forces and the assumption that $M_{xy} = M_{yx}$, the governing differential equation can be written as:

$$\tilde{h} \cdot \tilde{\rho} \cdot u_{tt} - (M^x_{xx} + 2 \cdot M^{xy}_{xy} + M^y_{yy}) = -F_b(x,y) + F_s(x,y,t), \quad (7)$$

with $F_b(x,y)$ the static force of the bridge, $F_s(x,y,t)$ the time varying force of the string course, and $\tilde{\rho} = \rho(x,y)$ the mass at the respective points on the soundboard. Figure 1 shows the geometry and the position of the ribs of the modeled soundboard.

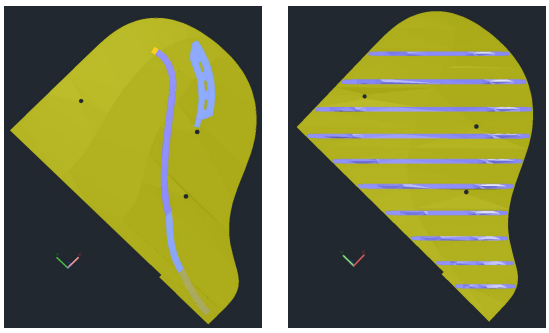

Figure 1: Geometry of the implemented grand piano soundboard, modeled after a Steinway grand piano.

2.4 Coupling model

The bridge of the piano acts as a transducer of string energy to the pianos soundboard. The exact properties of the bridge and its influence on the radiated sound is still under active research and there are indications that subtleties of a piano bridge have a direct influence on the sound of the piano [2]. The coupling from the string to the soundboard is implemented by an approximation of the transversal force at the interaction point. The force of a stiff string acting at the bridge can be written as:

$$F_{cp} = B \cdot u_{xxx} + T \cdot u_x, \quad (8)$$

with B the bending stiffness and T the tension of the string.

Because the impedance from the soundboard to the string is small, the coupling is approximated by a real mechanical impedance as $Z_{str} = \frac{F_{cp}}{v_{cp}}$ or reordered:

$$F_{cp} = Z_{str} \cdot v_{cp} \quad (9)$$

Although the assumption is not completely physically justifiable it is a feasible approximation over a certain frequency range.

3 Numerical model

The numerical solution of the system of differential equations is implemented with explicit finite difference schemes. The force of the hammer is calculated utilising a FDTD scheme [14]. The differential equation of the strings and the soundboard are semi-discretised to yield a number of coupled ordinary differential equation which can be integrated by the symplectic Euler algorithm as presented in by the author [28]. The methodology is as follows, 1) the differential equation without losses is semi-discretised in the spatial derivatives, 2) the terms for the losses are added, 3) the resulting system of coupled ordinary differential equations is iterated in time applying the sympectic Euler time integration scheme. As shown by Luo and Guo [1], energy losses can be added to the basic formulation of a symplectic integrator without the loss of overall accuracy of the method.

3.1 Finite difference operators

For reasons of brevity and compactness, a finite difference operator notation is applied in this work, similar to the notation used in Bilbao [14]. A discrete shift operator is indicated by ϵ with $\epsilon_{t-}u[t,k] = u[t-\Delta t,k]$ and $\epsilon_{x-}u(t,k) = u[t,k-\Delta x]$. A forward//backward difference approximation of a 1-dimensional vector $\mathbf{u}$ at position k can be written as:

$$\delta_{x+} = \frac{1}{\Delta x}(\epsilon_{x+} - 1) \Big|\Big| \delta_{x-} = \frac{1}{\Delta x}(1 - \epsilon_{x-}) \quad (10)$$

Higher order operators can be derived from these fundamental ones, i.e. $\delta_{xx} = \delta_{x-}\delta_{x+}$. A bold operator $\delta_{\mathbf{xx}}\mathbf{u}$ indicates that the operator is applied over the whole domain of $\mathbf{u}$ effectively resulting in a matrix vector multiplication.

3.2 Discrete hammer-string model

Utilising Newtons second law of motion, equation 1 can be rewritten as

$$x_{tt} = \frac{-F_0}{m}\left[(1-\zeta)\, x^\gamma + \tau x_t^\gamma\right] \quad (11)$$

with m the mass of the hammer head and the hammer shank. The differential term on the left side of the equality sign can be approximated numerically with a centered finite difference, the right side with a backward finite difference:

$$x_{tt} \approx \delta_{tt}x = \frac{-F_0}{m}\left[(1-\zeta)\, x^\gamma + \tau\delta_{t-}x^\gamma\right] \quad (12)$$

Reordering this equation to $\epsilon_+ x$ results in following scheme:

$$\epsilon_{t+}x = \frac{F_0}{m} \cdot \Delta t^2[(1-\zeta)\, x^\gamma + \tau x^\gamma(1-\epsilon_-)] - \epsilon_{t-}x + 2x \quad (13)$$

This equation can be iterated recursively in time by applying the initial conditions derived from the start velocity of the hammer and the other material parameters taken from [15].

3.2.1 Discrete string course

The semi-discretisation of the string is achieved by a partitioning the string $u \in 0, L$ into N parts. The transversal deflection of the string is calculated as:

$$\begin{bmatrix} \mathcal{A}_{sT} \\ \mathcal{V}_{sT} \\ \mathcal{U}_{sT} \end{bmatrix} = \bigcup_{t=1}^{T} \begin{Bmatrix} (\delta_{xx}(1-\alpha\delta_{t-}) - \kappa\delta_{4x}) \cdot [\epsilon_{t-}\mathbf{u}] - \beta\epsilon_{t-}\mathbf{v} \\ \epsilon_{t-}\mathbf{v} + \mathbf{a} \\ \epsilon_{t-}\mathbf{u} + \mathbf{v} \end{Bmatrix}. \quad (14)$$

Introducing $\mathcal{A}_{sT}, \mathcal{V}_{sT}, \mathcal{U}_{sT}$ the acceleration, velocity and the deflection of the transversal string motion over the complete spatial- and time domain. $\mathbf{a}, \mathbf{v}, \mathbf{u}$ are the acceleration, velocity and deflection over the spatial domain. $\bigcup$ is the discrete Hutchinson operator indicating a summation over the spatial- and time domain.

Similar to the approach used in [13], the longitudinal motion is discretised with a larger spatial stride because only the first few modes are of interest in the radiated sound. The integration scheme can be written similar to scheme 14, omitting the fourth-order term.

3.3 Discrete soundboard

The numerical scheme of the soundboard has a similar structure as the model for the string with the difference that it is discretised in two dimensions. The semi-discretised time integrator can be written as:

$$\begin{bmatrix} \mathcal{A} \\ \mathcal{V} \\ \mathcal{U} \end{bmatrix} = \bigcup_{t=1}^{T} \cdots \begin{cases} \delta_{\mathbf{XY}} \left[\tilde{\delta}_{\mathbf{XY}} \cdot [\epsilon_{t-}\mathbf{M}] (1 - \alpha \cdot \delta_t) - \beta \cdot \epsilon_{t-}\mathbf{v} \right] \\ \epsilon_{t-}\mathbf{v} + \mathbf{a} \\ \epsilon_{t-}\mathbf{u} + \mathbf{v} \end{cases}, \tag{15}$$

with $\tilde{\delta}_{\mathbf{XY}} = (D_x\delta_{xx} + D_y\delta_{yy} + 2(D_{xy} + 2D_s)\delta_{xy})$ weighted with the variable height, respective Young's moduli and Poisson ratios and a formulation for fixed boundary conditions at the rim of the soundboard and $\delta_{\mathbf{XY}} = (\delta_{xx} + \delta_{yy} + 2\delta_{xy})$.

4 Hardware implementation

The real-time version of the algorithm in hardware is achieved by implementing the finite difference scheme in the hardware description language VHDL. All core calculations of the algorithm are implemented with a fixed point Q0.31 two's-complement data type. As presented by the author [10], several beneficial features can be applied to accelerate the calculation of finite difference models using this data-type. As depicted in Figure 2 the physical model is implemented on two Virtex ML605 boards that are connected by coaxial cables. Board 2 is connected via a PCIe port to a standard PC. Figure 2 shows a block diagram of the implementation.

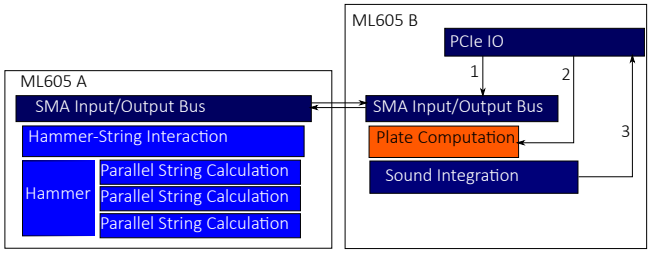

Figure 2: Block diagram of the FPGA model. 1) String/Hammer parameters. 2) Plate parameters. 3) Integrated sound.

In contrast to common Digital Signal Processing (DSP) chips or standard CPUs, which perform most calculations sequentially, FPGAs inherently have a parallel structure. Meaning, all logic resources on a FPGA compute the assigned logic functions at the same discrete time step. If one wants to implement sequential algorithms, particularly algorithms that depend on calculations from preceding time steps, a Finite Stat Machine (FSM) has to be implemented. The FSM ensures defined discrete computation steps with well-defined results at the end of a state.

4.1 Parallelization

The hardware implementation makes use of the parallel capabilities of the FPGA chip. To this end, the transversal calculation of the string is divided into parallel sub-calculation kernels of 10 discrete points which are computed in parallel. The requirements for a single discrete point of scheme 14, without the excitation function of the transversal motion are:

$$u = f(\epsilon_{t-}u, \epsilon_{t-}v, \epsilon_{x+}u, \epsilon_{x-}u, \epsilon_{x+}\epsilon_{x+}u, \epsilon_{x-}\epsilon_{x-}u). \tag{16}$$

The velocity v, and the deflection u of the preceding time step are saved in two memory positions which are loaded in the first FSM step depicted in Figure 3. The values for the deflection of the adjacent computation kernels are routed in the first step of the FSM as indicated by the horizontal arrows in Figure 3.

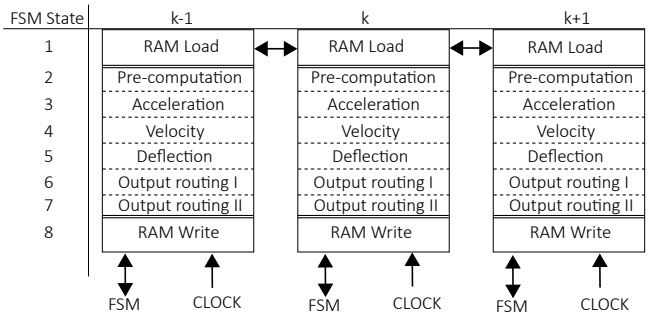

Figure 3: Three parallel computation kernels. The horizontal lines indicated the separate states of the calculation. The horizontal arrows indicate the data transfer between the kernels.

5 Results

Figure 4 shows the modeled hammer forces for varying initial velocities of the piano hammer showing the influence of different initial velocities of the hammer on the shape of the hammer force.

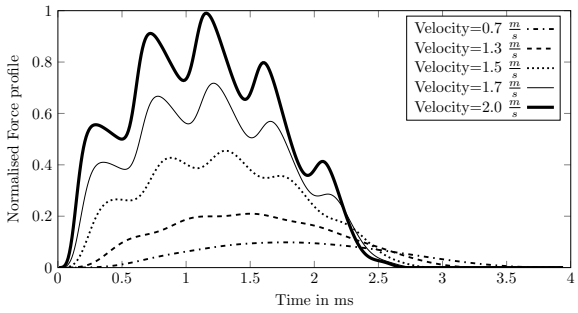

Figure 4: Simulated hammer forces with differing initial velocities.

Figure 5 shows a time series of three individual strings from the same course as a result to changing hammer positions on the string. This shows that the contact point between the hammer and the string can be changed while playing and the hammer can excite a string in motion without stopping the string calculation.

6 Conclusion

In this work, a functional real-time implementation of a string course consisting of three strings, excited by a hysteretic hammer model coupled to a orthotropic soundboard with realistic material- and geometrical properties was presented. The simulation results show good

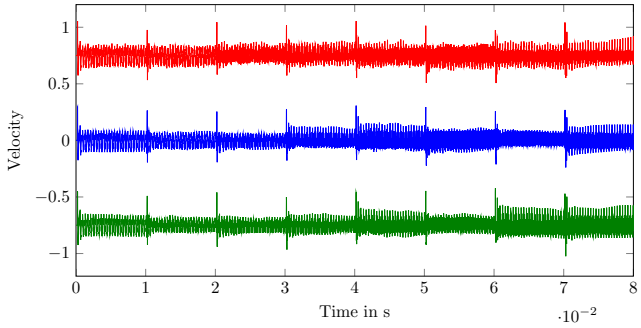

Figure 5: Velocity at the bridge with changing hammer positions .

agreement with measurements and comparable physical models of this particular system. The analysis of the hardware design regarding resource and area utilisation on the chip revealed that the soundboard can be implemented with a grid size of $80x64$ grid-points in real-time on a single Virtex-6 XCV240t FPGA chip. The complete set of strings for a 88 key grand piano, consisting of 200 single strings with a discretisation of 80-160 node points per string, is not computable in whole on one XVC240t FPGA chip.

The upcoming research project at the University of Hamburg in collaboration with Steinway Pianos, Hamburg is aimed at modeling and synthesizing a whole geometry model of a grand piano computed on more recent FPGA devices, in special Virtex-7 chips. When extrapolating the resource utilisation of a whole geometry design conservatively the model can be implemented on two Virtex-7 FPGAs. This implementation is part of an ongoing project and will be subject to future work.

Acknowledgments

I sincerely like to thank the *Deutsche Forschungs Gesellschaft* (DFG) which supported the development of the base system from 2010-2012. Furthermore, I would like to thank Mr. Stelter and Mr. Grube at Steinway Pianos Hamburg for the inspiring exchange of ideas.

References

[1] T. Luo, Y. Guo, "Application of Explicit Symplectic Algorithms to Integration of Damping Oscillators", *arXiv:1103.1455v1*

[2] Chabassier, Juliette and Chaigne, Antoine and Joly, Patrick, "Time domain simulation of a piano. Part 1 : model description.", *ESAIM: Mathematical Modelling and Numerical Analysis*, 1-20 (2013)

[3] A. Stulov , "Experimental and computational studies of piano hammers", *Acta Acustica united with Acustica* **91**, 1086–1097 (2005)

[4] X. Boutillon, K. Ege, and S. Paulello, "Comparison of the vibroacoustical characteristics of different pianos" in *11th Congrès Français d'Acoustique*, (2012)

[5] X. Boutillon, "Model for piano hammers: Experimental determination and digital simulation", *J. Acoust. Soc. Am.*, **83**(2), 746–754 (1988)

[6] A. Askenfelt and E. Jansson, "From touch to string vibrations—the initial course of the piano tone", *J. Acoust. Soc. Am.* **81**(S1), 61–61 (1987)

[7] A. Askenfelt, *Five Lectures on the Acoustics of the Piano*, ser. Publications issued by the Royal Swedish Academy of Music. Kungl. Musikaliska Akademien, 1990.

[8] B. Bank and H.-M. Lehtonen, "Perception of longitudinal components in piano string vibrations", *J. Acoust. Soc. Am.*, **128** (3), 117–123, 2010.

[9] N. Giordano and A. J. Korty, "Motion of a piano string: Longitudinal vibrations and the role of the bridge", *J. Acoust. Soc. Am.* **100**(6), 3899–3908 (1996)

[10] F. Pfeifle, "Real-time finite difference physical models of musical instruments on a Field Programmable Gate Array (FPGA)", in *Proc. of the Int. Conf. on Digital Audio Effects (DAFx-12)*, York, UK, Sept. 17–21, 63–70 (2012)

[11] S. Birkett, "Experimental investigation of the piano hammer-string interaction", *J. Acoust. Soc. Am.* **133**(4), 2467–2478 (2013)

[12] A. Stulov, Hysteretic model of the grand piano hammer felt, *J. Acoust. Soc. Amer.* **97**, 2577-2585 (1995)

[13] B. Bank, L. Sujbert, "Modeling the longitudinal vibration of piano strings", in *Proc. Stockholm Music Acoust. Conf.*, Stockholm, Sweden (2003), 143–146

[14] S. Bilbao, *Numerical Sound Synthesis: Finite Difference Schemes and Simulation in Musical Acoustics.*, John Wiley and Sons, Chichester (2009)

[15] A. Stulov, "Experimental and theoretical studies of piano hammer", in *Proceedings of the Stockholm Music Acoustics Conference*, 2003.

[16] N. H. Fletcher and T. D. Rossing, *The Physics of Musical Instruments*. Springer Verlag, 1998.

[17] A. Chaigne and A. Askenfelt, "Numerical simulations of piano strings. I. a physical model for a struck string using finite difference methods", *J. Acoust. Soc. Am.* **95**(2) , 1112–1118 (1994)

[18] ——, "Numerical simulations of piano strings. II. comparisons with measurements and systematic exploration of some hammer-string parameters," *J. Acoust. Soc. Am.*, **95**(3), 1631–1640, (19940

[19] A. Mamou-Mani, J. Frelat, C. Besnainou, "Numerical simulation of a piano soundboard under downbearing", *J. Acoust. Soc. Am.* **123**(4), 2401–2406 (2008)

[20] A. Mamou-Mani, S. L. Moyne, F. Ollivier, C. Besnainou, and J. Frelat, "Prestress effects on the eigenfrequencies of the soundboards: Experimental results on a simplified string instrument", *J. Acoust. Soc. Am.* **131**(1), 872–877 (2012)

[21] V. Bucur, *Acoustics of Wood*, Springer, Berlin (2006)

[22] J.A. Gibbons, D.M. Howard, A.M. Tyrrell, "FPGA implementation of 1D wave equation for real-time audio synthesis", *IEEE Proceedings, Computers and Digital Techniques* **152** (5), 619-631 (2005)

[23] W. Chen, P. Kosmas, M. Leeser, C. Rappaport, "An FPGA implementation of the two-dimensional finite-difference time-domain (FDTD) algorithm" *Proceedings of the 2004 (ACM/SIGDA) 12th international symposium on Field programmable gate arrays*, New York, 213-222 (2004)

[24] B. Bank, L. Sujbert, "Generation of longitudinal vibrations in piano strings: From physics to sound synthesis", *J. Acoust. Soc. Am.* **117**(4), 2268-2278 (2005)

[25] J. Bensa, S. Bilbao, R. Kronland-Martinet, J.O. Smith , "The simulation of piano string vibration: From physical models to finite difference schemes and digital waveguides" *J. Acoust. Soc. Am.* **114**(2), 1095-1107 (2003)

[26] E. Motuk, R. Woods, S. Bilbao, "Implementation of Finite-Differece Schemes for the Wave Equation on FPGA" *IEEE International Acoustics Speech and Signal Processing ICASSP 2005* **3**, (2005)

[27] E. Motuk, R. Woods, S. Bilbao, J. McAllistere, "Design Methodology for Real-Time FPGA-Based Sound Synthesis" *IEEE Transactions on signal processing* **55**(12), (2007)

[28] F. Pfeifle , "Multisymplectic Pseudo-Spectral Finite Difference Methods for Physical Models of Musical Instruments" in *Sound - Perception - Performance* **1**, Springer, 351-365 (2013)

[29] D. Russel, T. Rossing, "Testing the Nonlinearity of Piano Hammers Using Residual Shock Spectra", *Acustica* **84**, 967-975 (1998)

[30] R.A. Bacon, J.M. Bowsher, "A discrete model of a struck string", *Acustica* **41**, 21-27 (1978)